Influences of cracking of coated superconducting layer on voltage-current curve, critical current, and *n*-value in DyBCO-coated conductor pulled in tension

S. Ochiai,[1,a)] T. Arai,[1] A. Toda,[1] H. Okuda,[1] M. Sugano,[2] K. Osamura,[3] and W. Prusseit[4]
[1]*Department of Materials Science and Engineering, Kyoto University, Sakyo-ku, Kyoto 606-8501, Japan*
[2]*Department of Electronic Science and Engineering, Kyoto University, Kyoto-Daigaku Katsura, Nishikyo-ku, Kyoto 615-8530, Japan*
[3]*Research Institute for Applied Sciences, Sakyo-ku, Kyoto 606-8202, Japan*
[4]*THEVA Dünnschichttechnik GmbH, Rote-Kreuz-Straße 8, 85737 Ismaning, Germany*

(Received 23 June 2010; accepted 9 August 2010; published online 17 September 2010)

Influences of cracking of coating layer under applied tensile strain on *V*(voltage)-*I*(current) curve, critical current, and *n*-value of $DyBa_2Cu_3O_{7-\delta}$ coated conductor were studied experimentally and analytically. The experimentally measured variations in *V*-*I* curve, critical current, and *n*-value with increasing applied strain and the correlation of *n*-value to critical current were described well by the partial crack-current shunting model of Fang *et al.* Also, the variations in the ratio of shunting current to overall critical current and the ratio of voltage developed in the cracked region to overall voltage with extension of crack, and the variation in critical current with the ratio of noncracked area to overall cross-sectional area of superconducting layer were revealed. © *2010 American Institute of Physics*. [doi:10.1063/1.3488014]

I. INTRODUCTION

$Re(Y,Sm,Dy)Ba_2Cu_3O_{7-\delta}$ coated conductors with long length and high critical current have been developed and are expected for wide application such as power cables, fault current limiters and current leads.[1–4] In fabrication and service, they are, more or less, subjected to thermal, mechanical, and electromagnetic stresses/strains. Concerning the influence of subjected strain on critical current of coated conductors, it has been revealed that the critical current is reversible up to the irreversible strain at which cracking occurs in the $ReBa_2Cu_3O_{7-\delta}$ layer but beyond the irreversible strain, the critical current decreases with increasing applied strain due to the extension of cracking.[5–14] It is required to reveal the relation of cracking to superconducting properties for safe and reliability in application. In the present work, we studied the influence of cracking of the superconducting layer on the critical current and *n*-value in the $DyBa_2Cu_3O_{7-\delta}$ (DyBCO) coated conductor with MgO buffer layer deposited on the Hastelloy C-276 substrate by inclined substrate deposition (ISD), prepared at THEVA, Germany.[15] Compared to YBCO, DyBCO has the advantages of a better chemical stability and more resistance to corrosive ambient, a slightly higher transition temperature, and a lower surface resistance at 77 K.[16]

The as-supplied conductor had been coated with a thin Ag layer of 0.5 μm to solder the voltage taps for measurement of *V*(voltage)-*I*(current) curve and critical current under no applied strain. Sugano *et al.*[5,6] have revealed, when the Hastelloy C-276 is exposed at the deposition temperature (963 K in this case), discontinuous yielding takes place similarly to the Lüders band extension under applied strain, causing arrayed multiple cracking of the coated layer and hence causing reduction in critical current. An example of the arrayed multiple cracking in the DyBCO layer, observed in the present sample is shown in Fig. 1. The cracks are small in the initial stage of multiple cracking but it extends in transverse direction with increasing applied strain. Sugano *et al.*[5,6] have also found that quenching occurs after several percent-reduction in critical current, due to the progress of multiple cracking and small thickness of Ag layer. This premature quenching makes it difficult to measure the strain-dependence of critical current in wide strain range that covers the variation in critical current from the original value to zero.

In the present work, copper was electroplated onto the sample in order to give a shunting circuit that acts when the imposed current encounters the cracks. With copper plating,

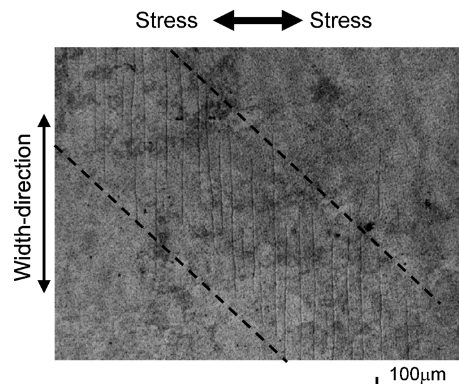

FIG. 1. An example of the arrayed multiple cracking of the DyBCO layer, observed in the copper-plated sample used in the present work. The appearance of the cracked DyBCO layer was observed by etching away the copper and silver layers after application of tensile strain on the sample.

a)Electronic mail: shojiro.ochiai@materials.mbox.media.kyoto-u.ac.jp.

 © 2010 American Institute of Physics

Downloaded 25 Nov 2010 to 130.54.110.31. Redistribution subject to AIP license or copyright; see http://jap.aip.org/about/rights_and_permissions

the change in critical current from the original value to zero with increasing applied tensile strain could be measured successfully. The measured changes in *V-I* curve, critical current I_c, and *n*-value with increasing applied strain and the obtained correlation of *n*-value to critical current are shown in Sec. III. The experimental results were analyzed by the model of Fang *et al.*[17] The outline of the model is shown in Sec. IV. The result of the analysis is shown in Sec. V. It is shown that the experimental results are described well by this model. Also the variations in critical current, shunting current, and voltage developed in the cracked region with extension of crack are discussed.

II. EXPERIMENTAL DETAILS

A. Sample

The DyBCO coated conductor prepared by THEVA was used for the present experiment and analysis. The fabrication procedure has been shown elsewhere.[15] The sample consisted of Hastelloy C276 substrate (thickness 90 μm), MgO buffer layer (3.3 μm) deposited by ISD process, MgO cap layer (0.3 μm), DyBCO superconducting layer (2.5 μm), and Ag contact layer (0.5 μm). The width of the conductor was 10 mm. Due to the reason mentioned in Sec. I, copper was electroplated onto the sample at room temperature with an electrolyte composed of $CuSO_4$:210 g/l, H_2SO_4:52.4 g/l and pure water. The thickness of the plated copper layer was 35 μm.

B. Measurement of *V-I* curve, critical current I_c, and *n*-value of copper plated-sample under applied tensile strain

Tensile strain was applied to the sample at 77 K with an Instron type testing machine. The sample was gripped by copper chucks, which also worked as current electrodes during measurement of critical current. To reduce the stress concentration within and near the chucks, Indium foils were inserted between the sample and chucks. For measurement of strain of the sample, a couple of very light Nyilas[18] type extensometers were attached directly to the sample.

The voltage taps for measurement of the *V-I* curves were soldered with a spacing of 45 mm. The *V-I* curves under various applied strains were measured with the usual four-probe method at 77 K under a self magnetic field. The *V-I* curve was approximated by

$$V = AI^n, \tag{1}$$

where *n* and *A* are the fitting constants. The *n*-value was estimated for the voltage range of $V=0.1-10$ μV/cm. The critical current I_c was estimated with a criterion of 1 μV/cm.

III. MEASURED *V-I* CURVES, CRITICAL CURRENT I_C, AND *N*-VALUES UNDER APPLIED TENSILE STRAIN

Figure 2(a) shows the change in measured critical current I_c and *n*-value with increasing applied tensile strain ε_T. The correlation of *n*-value to critical current I_c is shown in Fig. 2(b). Both I_c and *n*-value decreased significantly at high ε_T [Fig. 2(a)] due to the cracking of the DyBCO layer (Fig. 1). The lower the I_c, the lower became the *n*-value [Fig. 2(b)].

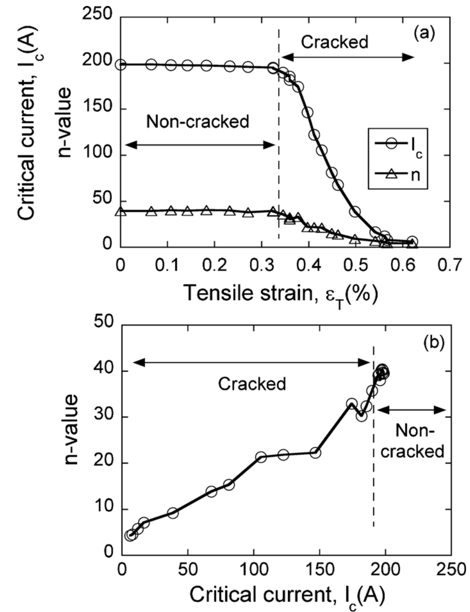

FIG. 2. Experimental results. (a) Change in critical current I_c and *n*-value with increasing applied tensile strain ε_T. (b) Plot of *n*-value against I_c.

The variation I_c as a function of ε_T in the reversible strain range has been investigated for wide variety of Re(Y, Sm, Dy)BCO samples.[5–14] The reported results show that the shape of $I_c-\varepsilon_T$ curve is dependent on the species of Re(Y, Dy, Sm), fabrication process and microstructure, residual strain and so on. Concerning the present DyBCO sample in the as-supplied state (without cupper plating), it has been shown that I_c decreases almost linearly.[5,6] Fig. 3 shows the change in (a) critical current I_c and (b) *n*-value with increas-

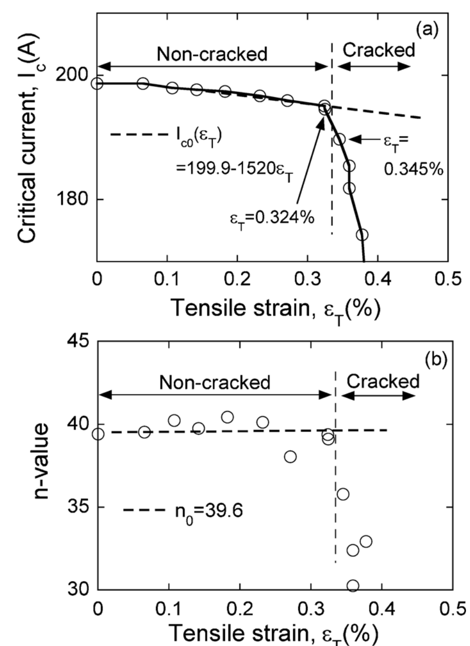

FIG. 3. Change in (a) critical current I_c and (b) *n*-value with increasing applied tensile strain ε_T in low tensile strain range.

Downloaded 25 Nov 2010 to 130.54.110.31. Redistribution subject to AIP license or copyright; see http://jap.aip.org/about/rights_and_permissions

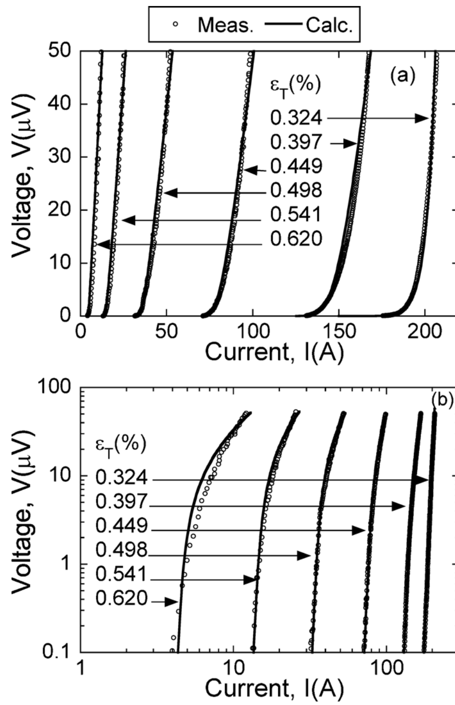

FIG. 4. Representative examples of the *V-I* curves in (a) normal and (b) logarithmic scale. Open circles show the experimental results. Solid curves show the calculation results with the procedure shown in Sec. IV.

ing ε_T in low tensile strain range of the present copper-plated DyBCO sample. In Fig. 3(a), I_c decreased almost linearly with ε_T in the tensile strain range of $0.1\% < \varepsilon_T < 0.324\%$ and it decreased sharply at the next strain $\varepsilon_T = 0.345\%$. In Fig. 3(b), the change in *n*-value with ε_T up to $\varepsilon_T = 0.324\%$ was minor in comparison with the sharp decrease at $\varepsilon_T = 0.345\%$. These results suggest that the irreversible tensile strain, $\varepsilon_{T,irr}$, existed between 0.324% and 0.345%, as indicated in Fig. 3(a). The sharp decreases in I_c and *n*-value beyond $\varepsilon_T = 0.324\%$ stem from cracking in the DyBCO layer. The ranges of ε_T in noncracked and cracked states in the present copper-plated sample are shown in Fig. 3(a) and 3(b).

A monotonic decrease in I_c with ε_T was found in the strain range of around $0.1\% < \varepsilon_T < 0.324\%$ in the present sample. Hereafter, we focus on the strain range of $0.1\% < \varepsilon_T$. The strain dependence of critical current I_{c0} in noncracked range of $0.1\% < \varepsilon_T < 0.324\%$ was approximated by

$$I_{c0} = 199.9 - 15.20\varepsilon_T. \tag{2}$$

The strain dependence of *n*-value in the noncracked range was not large as in Fig. 3(b). Thus, the *n*-value in noncracked range was given by the average of the *n*-values measured in this range, $n_0 = 39.6$. The I_{c0} given by Eq. (2) and $n_0 (=39,6)$ are used for analysis of the experimental results of *V-I* curve, I_c, and *n*-value in Secs. IV and V.

Figure 4 shows representative examples of the measured *V-I* curves in (a) normal and (b) logarithmic scale. The Open circles show the experimental results. The *V-I* curve measured at $\varepsilon_T = 0.324\%$ refers to noncracked state and the *V-I* curves measured at other strains refer to cracked-state. Solid curves show the calculation results with the model of Fang *et al.*,[17] whose outline is shown below.

IV. MODEL USED FOR ANALYSIS

The influence of shunting of current under an existent partial crack in a $Bi_2Sr_2Ca_2Cu_3O_{10+\delta}$ (BSCCO) filament embedded in stabilizer on the *V-I* relation has been modeled by Fang *et al.*[17] Here, "partial crack" means the crack that exists in a part of transverse cross-section of the superconducting filament. Shin *et al.*[19] have applied this model to the measured *V-I* curves of the BSCCO filamentary composite tape under applied tensile strain. They found that the measured *V-I* curves and change in I_c as a function of ε_T can be described with this model by using an effective relative crack size (ratio of the cracked cross-sectional area to overall transverse cross-sectional area). Miyoshi *et al.*[20] have applied this model to the *V-I* curves of the Nb_3Sn filamentary composite tape containing collective cracks (cracks composed of successively fractured filaments in a transverse cross-section). They found a linear relationship between the relative size of the collective crack and crack density and found that this model captures the effect of diminishing I_c as a function of fractional decrease in the number of intact filaments. In the present work, we use this model, originally proposed to analyze the influence of a partial crack in a BSCCO filament, for analysis of *V-I* curve and for estimation of critical current I_c and *n*-value in the present coated conductor, since the shunting mechanism under existent cracks is common in both filamentary and coated conductors despite the difference in geometry.

In the present sample, the stabilizer contact to DyBCO layer is composed of silver (0.5 μm in thickness) and plated copper (35 μm) layers. Figure 5 shows a schematic representation of (a) current path, (b) electrical circuit, and (c) simplified electrical circuit under an existent partial crack in DyBCO layer. In the transverse cross-section in which a partial crack exists [Fig. 5(a)], the cracked part losing superconductivity and noncracked part keeping superconductivity coexist. We define the ratio of cross-sectional area of cracked part to overall cross-sectional area of DyBCO layer as f. The noncracked part with an area ratio $1-f$ transports current I_d through DyBCO layer [Fig. 5(b)]. At the cracked part with an area ratio f, current I_s $(=I-I_d)$ shunts into Ag and Cu layers [Fig. 5(b)]. In the shunting circuit in Fig. 5(b), the R_{e1} and R_{e2} refer to the resistances at the DyBCO–Ag and Ag–Cu interfaces, respectively, and R_{Ag} and R_{Cu} to the resistances in Ag and Cu, respectively. The shunting currents that go through Ag and Cu are noted as I_{Ag} and I_{Cu}, respectively. The total shunting current I_s is the sum of I_{Ag} and I_{Cu}. In (c), the total resistance in the shunting circuit in (b) is replaced by R_t. The voltage developed in the noncracked part that transports current I_d is noted as V_d in (b) and (c). The voltage $V_s = I_s R_t$ developed in the cracked part by shunting current I_s is equal to V_d in (c) since the noncracked and cracked parts constitutes of a parallel circuit.

The *V-I* relation of noncracked DyBCO layer with a critical current I_{c0} given by Eq. (2) is expressed as

Downloaded 25 Nov 2010 to 130.54.110.31. Redistribution subject to AIP license or copyright; see http://jap.aip.org/about/rights_and_permissions

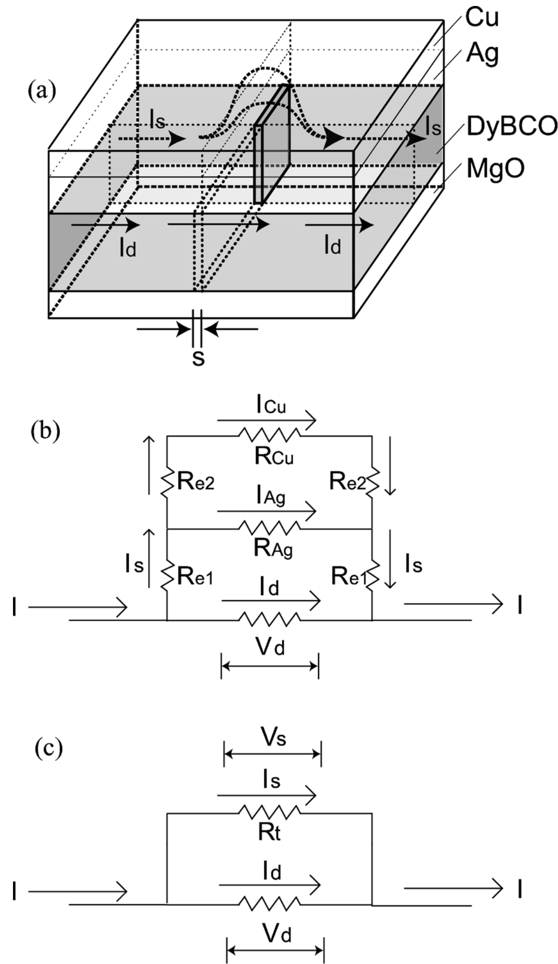

FIG. 5. Schematic representation of (a) current path, (b) electrical circuit and (c) simplified electrical circuit under an existent crack. In (c), the total resistance in the shunting circuit shown in (b) is replaced by R_t.

$$V = E_c L \left(\frac{I}{I_{c0}} \right)^{n_0}, \tag{3}$$

where L is the distance between the voltage taps (45 mm in the present work), E_c is the electric field criterion for critical current (1 μV/cm), and n_0 is the n-value in noncracked state.

The voltage V_d developed in the noncracked part in a partially cracked cross-section is expressed as

$$V_d = E_c s \left\{ \frac{I_d}{I_{c0}(1-f)} \right\}^{n_0}, \tag{4}$$

where s is the crack width [Fig. 5(a)]. In calculation, s was taken to be 0.1 μm as in the preceding works.[17,19,20] The influence of s-value on the result of analysis is discussed in Sec. V D. The voltage V_d in Eq. (4) is equal to V_s ($=I_s R_t$), as stated above. The overall current I is the sum of I_d and I_s. By substituting I_d derived from Eq. (4) and $I_s = V_d / R_t$ into $I = I_d + I_s$, I is expressed as

$$I = I_{c0}(1-f) \left(\frac{V_d}{E_c S} \right)^{1/n_0} + \frac{V_d}{R_t}. \tag{5}$$

The overall voltage V is given by the sum of the voltage along the length of $L-s$ in the noncracked region and the length s in the cracked region. As s (0.1 μm) is small enough in comparison with L (45 mm), the overall voltage V is expressed as

$$V = E_c L \left(\frac{I}{I_{c0}} \right)^{n_0} + V_d. \tag{6}$$

In application of this model to the present experimental result, the arrayed cracks (Fig. 1) were treated as a single equivalent crack, since the shunting of current occurs in the same mechanism in both single and multiple cracks. Accordingly, the values of f and R_t obtained by fitting Eqs. (5) and (6) with the measured V-I curves correspond to the total effect of multiple cracks. As shown in Sec. V below, the experimental results are described well by the replacement of multiple cracks by a single equivalent crack, indicating that the present approach is useful for analysis of arrayed cracks with complex geometry that appear in most coated conductors especially at high applied strain.

V. RESULT OF ANALYSIS AND ITS COMPARISON WITH EXPERIMENTAL RESULTS

A. Obtained values of $1-f$ and R_t and comparison of the calculated V-I curves, I_c, and n-values with experimental results

As the cracking occurred beyond $\varepsilon_T = 0.324\%$, it was impossible to measure the critical current I_{c0} and n_0-value under no crack for $0.324\% < \varepsilon_T$. As an approximation, the I_{c0} value obtained by the extrapolation of Eq. (2) to each tested $\varepsilon_T (>0.324\%)$ was used for analysis. n_0-value beyond $\varepsilon_T = 0.324\%$ was taken to be 39.6 (Fig. 3). Substituting $L = 45$ mm, $s = 0.1$ μm, $n_0 = 39.6$, and I_{c0} [obtained by substituting the corresponding ε_T into Eq. (2)] into Eqs. (5) and (6), and fitting the experimentally measured V-I curve (Fig. 4) with Eqs. (5) and (6), we had the ratio $1-f$ of noncracked area to overall cross-sectional area of DyBCO layer and the resistance R_t in the cracked range of $0.324\% < \varepsilon_T$. The $1-f$ was taken to be unity in the noncracked range of $0.1\% < \varepsilon_T < 0.324\%$. The obtained values of $1-f$ and R_t are plotted against applied tensile strain ε_T in Fig. 6. In the cracked range of $0.324\% < \varepsilon_T$, the $1-f$ decreased from unity to almost zero and the R_t tended to increase with ε_T due to the crack extension.

The obtained values of $1-f$ and R_t were substituted into Eqs. (5) and (6), and the V-I curve at each ε_T was back-calculated. Examples of the calculated V-I curves are shown in Fig. 4. The experimental results are described well, as expected. From the calculated V-I curve with the estimated $1-f$ and R_t values, the critical current I_c under 1 μV/cm criterion and n-value in the voltage range of 0.1–10 μV/cm were calculated. Figure 7 shows the comparison of the experimental results (open circles) with the calculation results (open triangles) for (a) critical current I_c, (b) n-value, and (c) correlation between n-value to I_c. The experimental results are well described by the calculation results. As stated in Sec. IV, in application of the model of Fang et al.[17] to the present experimental result, the arrayed cracks (Fig. 1) were treated as a single equivalent crack. The good agreement of calculation results with experimental results for V-I curves,

Downloaded 25 Nov 2010 to 130.54.110.31. Redistribution subject to AIP license or copyright; see http://jap.aip.org/about/rights_and_permissions

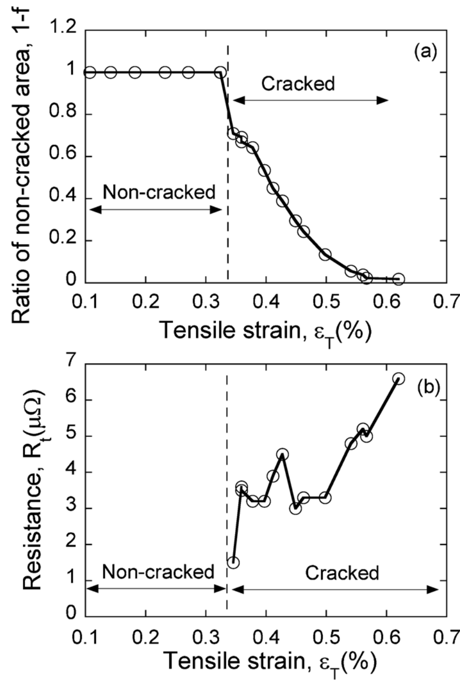

FIG. 6. Obtained values of (a) ratio of noncracked area $1-f$ and (b) resistance R_t in the shunting circuit, plotted against applied tensile strain ε_T.

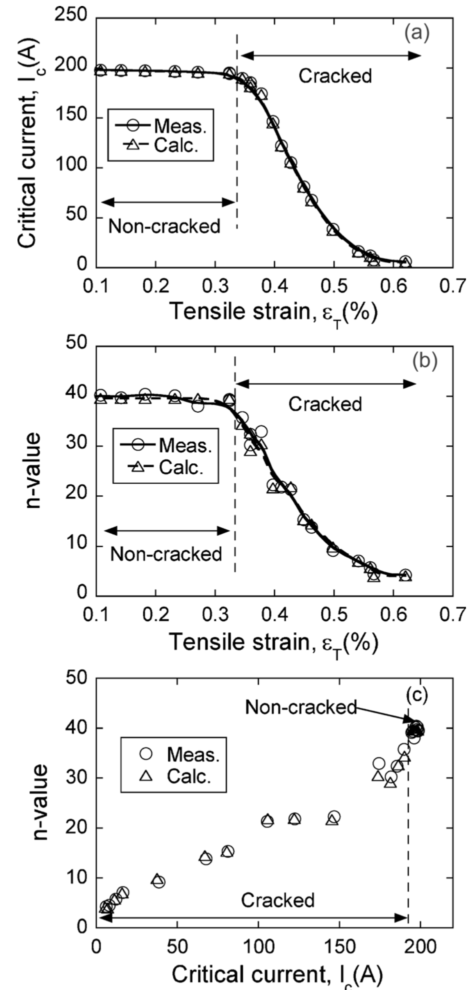

FIG. 7. Comparison of the experimental results with the calculation results by Eqs. (5) and (6) with the obtained $1-f$ and R_t values. (a) Change in critical current I_c with applied tensile strain ε_T. (b) Change in n-value with ε_T. (c) Correlation between n-value to I_c.

I_c, n-value, and correlation of n-value to I_c indicates that the conversion of arrayed multiple cracks to a single equivalent crack can give a good description of superconducting properties and is useful for analysis of influence of cracking of superconducting layer on *V-I* behavior in coated conductors as well as for analysis of that in filamentary conductors.[19,20]

B. Shunting current I_s and voltage $V_s(=V_d)$ developed in the cracked region at $I=I_c$

Figure 8(a) shows an example of the measured and analyzed *V-I* curve and variation in shunting current I_s with overall current I. In this example, the data at $\varepsilon_T=0.411\%$ is picked up representatively. The values of $1-f$ and R_t, obtained by fitting Eqs. (5) and (6) to the measured *V-I* relation, were 0.451 $\mu\Omega$ and 3.89 $\mu\Omega$, respectively. The *V-I* curve back-calculated by Eqs. (5) and (6) with the obtained values of $1-f$ and R_t is shown with a solid curve. The shunting current I_s as a function of overall current I, calculated by $V_s(=V_d)/R_t$, is shown with a broken curve. The part indicated as (b) in Fig. 8(a) is shown in Fig. 8(b) at high magnification. The critical current I_c for the present voltage probe distance $L=45$ mm is defined at $V=V_c=4.5$ μV under the 1 μV/cm criterion. I_s increases with increasing overall current I, especially beyond $I=I_c$. The measured critical current, $I_{c,meas}$, was 122.4 A. The calculated critical current at $V=V_c=4.5$ μV was 122.1 A, which is very close to the measured value of 122.4 A. As shown in this example and as has been shown in Fig. 7, the difference between the calculated and measured I_c value at each ε_T was almost within 1 A. The calculated shunting current I_s at the calculated I_c at $V=V_c$ was 1.2 A. The ratio of I_s to I_c at $V=V_c$, I_s/I_c, was 0.01 in this example. In the same way, the I_s/I_c at $V=V_c$ at each measured ε_T was calculated and plotted against calculated I_c, as shown in Fig. 8(c). In the wide range of I_c (20–195 A, where 195 A is the critical current I_c at $\varepsilon_T=0.324\%$ just before the occurrence of cracking), the I_s/I_c was less than 0.05. This result indicates that most of the current (more than 95% of the imposed current) is transported by DyBCO layer at $I=I_c$ in the wide range of I_c values.

Figure 9(a) shows also examples of variation in overall voltage V and voltage at cracked part $V_s(=V_d)$ with overall current I, from which the value of V_s at $I=I_c$ ($V=V_c$ $=4.5$ μV), is read. In these examples, the calculated values of $V_{s,cal}$ were 3.42 μV and 4.50 μV at $\varepsilon_T=0.359\%$ and 0.411%, respectively. The ratios of V_s developed at cracked part to overall voltage V_c (4.50 μV) at $I=I_c(V=V_c)$ were 0.76 and 1.00 at $\varepsilon_T=0.359\%$ and 0.411%, respectively. In the same way, the V_s/V_c at $I=I_c$ at each ε_T was calculated and plotted against calculated I_c, as shown in Fig. 9(b). In the wide range of I_c (20–180 A), corresponding to the range of $0.359\% < \varepsilon_T$, the value of V_s/V_c was 1.00. This result shows that the overall voltage at $I=I_c$ in the cracked sample stems mostly from the cracked region.

The results in Figs. 8 and 9 show that, at $I=I_c$, most of the imposed current is transported by the noncracked part of the superconducting layer and the voltage is developed mostly in the cracked region in advance of development of

Downloaded 25 Nov 2010 to 130.54.110.31. Redistribution subject to AIP license or copyright; see http://jap.aip.org/about/rights_and_permissions

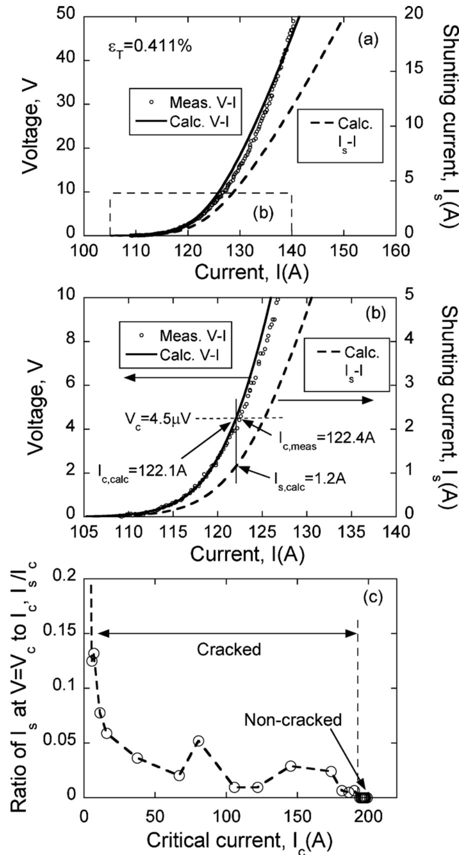

FIG. 8. (a) An example of measured and analyzed *V-I* curve and variation in shunting current I_s with overall current I. The portion (b) indicated in (a) is presented at high magnification in (b). (c) Ratio of I_s at $V=V_c$ to critical current I_c and I_s/I_c, showing that most of the current (more than 95%) is transferred by DyBCO layer at $I=I_c$ in the wide range of I_c values (20–195 A).

voltage in the noncracked region. These results suggest that the ratio $1-f$ of the noncracked area to overall cross-sectional area of the DyBCO layer plays a dominant role in determination of critical current. In the subsection below, the relation of I_c to $1-f$ is discussed.

C. Relation of critical current I_c to the ratio $1-f$ of noncracked area and voltage probe distance L

The $1-f$ values obtained by fitting Eqs. (5) and (6) to the measured *V-I* curves have been shown in Fig. 6(a). In order to examine whether the I_c value is proportional to $1-f$ or not, the measured I_c values are plotted against $1-f$, as shown in Fig. 10. The I_c increases with increasing $1-f$, demonstrating that $1-f$ plays a dominant role in determination of I_c. However, the following inconsistency is found in Fig. 10. I_c increases linearly with increasing $1-f$ up to around $1-f=0.7$. At $1-f=0.7$, I_c reaches almost the nondamaged value. This means that, even though the cross-sectional area that transports superconducting current is reduced by 30%, the critical current of nondamaged state is retained. This inconsistency is overcome as follows, by incorporating the influence of sample length L on I_c.

As shown in Sec V B. above, even under existence of crack, I_s/I_c is low (less than 0.05 in the wide range of I_c =20–195 A) at $V=V_c$ [Fig. 8(c)]. Also $V_s(=V_d)$ is almost the same as V_c in the wide range of I_c=20–180 A [Fig. 9(b)]. As a rough approximation, substituting $I_s(=V_d/R_t)=0$ A, $V_s=V_d=V_c(=E_cL)$, and $I=I_c$ into Eq. (5), we have

$$I_c = I_{c0}(1-f)\left(\frac{L}{s}\right)^{1/n_0}. \tag{7}$$

The term $(1-f)$ $(L/s)^{1/n_0}$ is, hereafter, called as a modified ratio of noncracked area, in which $1-f$ is modified with the ratio L/s of voltage probe distance (L) to crack width (s) and n_0-value. *V-I* curve is determined by Eqs. (5) and (6), and accordingly *V-I* curve is affected by the value of L that is included in the term $E_cL(I/I_{c0})^{n_0}$ in Eq. (6). However, under existence of crack, $E_cL(I/I_{c0})^{n_0}$ is far smaller than $V_d(=V_s)$ in Eq. (6) except when crack is very small, as representatively

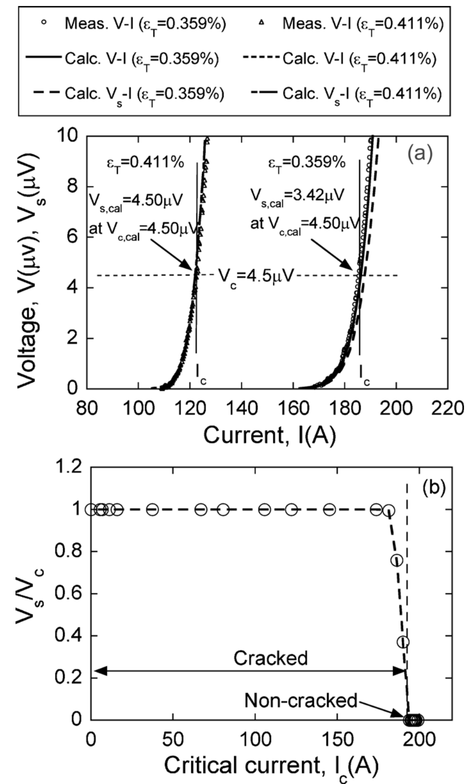

FIG. 9. (a) Examples of variation in overall voltage V and voltage at cracked region V_s with current I, from which the ratio V_s/V_c at $I=I_c$, is read. (b) Variation in V_s/V_c with critical current I_c, showing that the voltage stems from the cracked region in the wide range of I_c values (20–180 A).

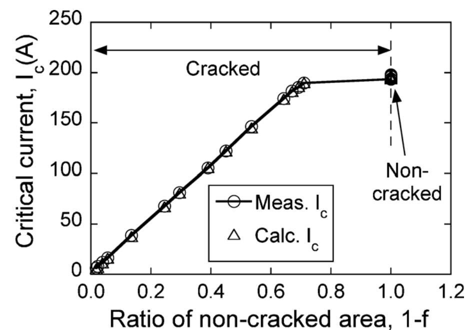

FIG. 10. Critical current (I_c) values plotted against the ratio of noncracked area $1-f$.

Downloaded 25 Nov 2010 to 130.54.110.31. Redistribution subject to AIP license or copyright; see http://jap.aip.org/about/rights_and_permissions

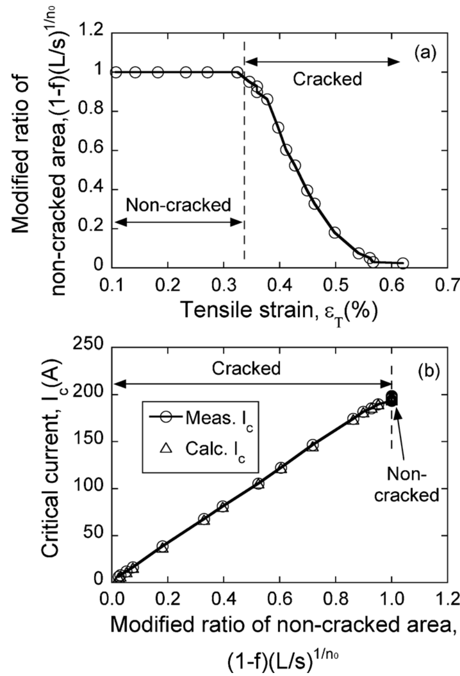

FIG. 11. (a) Modified ratio of noncracked area $(1-f)(L/s)^{1/n_0}$ plotted against tensile strain ε_T.(b) Critical current (I_c) values plotted against the modified ratio of noncracked area $(1-f)(L/s)^{1/n_0}$.

shown by $V_s/V_c=1$ in wide range of I_c in Fig. 9(b). Therefore, the influence of L on V-I curve is very small under existence of crack; namely, V-I curve is practically determined by the cracked region regardless of value of L. On the other hand, the critical current under a criterion of $V_c=E_cL$ is dependent on L; the larger the L, the higher becomes I_c for a given V-I curve. Such a feature of dependence of I_c on L under existence of crack is expressed by Eq. (7).

The modified ratio $(1-f)(L/s)^{1/n_0}$ of noncracked area, calculated with the $1-f$ values shown in Fig. 6(a), and $L=45$ mm, $s=0.1$ μm and $n_0=39.6$ which were used for obtaining $1-f$ values, is plotted against ε_T in Fig. 11(a). As the model used for analysis is constructed under the condition where I_c is reduced by cracking, I_c value under existence of crack is always lower than I_{c0} and hence $(1-f)(L/s)^{1/n_0}$ ranges from zero to unity, never exceeding unity. As has been shown in Fig. 6(a), the $1-f$ drops suddenly from unity to around 0.7 when cracking occurs, which is reflected in the range of constant critical current for $1-f\approx 0.7$ to 1.0 in Fig. 10. In contrast to the sudden drop in $1-f$ in Fig. 6(a), the modified ratio $(1-f)(L/s)^{1/n_0}$ decreases gradually. Also the critical current under existence of crack is almost proportional to $(1-f)(L/s)^{1/n_0}$, as shown in Fig. 11(b).

The result shown above means that, when cracking occurs very locally as in the present case, the V-I curve itself is determined almost by the very narrow cracked region whatever the value of L (=voltage probe distance/sample length) is, while the criterion $V_c=E_cL$ for I_c is dependent on L. In such a case, the modified ratio of noncracked area $(1-f)\times(L/s)^{1/n_0}$ is a useful parameter for description of I_c.

D. Influence of *s*-value on the result of analysis

In the present work, $s=0.1$ μm was used as similarly as in the preceding works for BSCCO and Nb_3Sn conductors.[17,19,20] However, whether $s=0.1$ μm is suitable for the present DyBCO conductor or not is not sure. In this subsection, the influence of s-value on the result of analysis is discussed below. It is shown that, even when s-value other than 0.1 μm is used, the analyzed results of V-I curve, I_c, n-value, shunting behavior are the same as those obtained for $s=0.1$ μm, while the value of $1-f$ becomes different, depending on s-value.

Equation (5) is rewritten in the following modified form:

$$I = I_{c0}(1-f)\left(\frac{L}{s}\right)^{1/n_0}\left(\frac{V_d}{E_cL}\right)^{1/n_0} + \frac{V_d}{R_t}. \tag{8}$$

In Eq. (8), only the expression is changed from that in Eq. (5), as to include the modified ratio of noncracked area $(1-f)(L/s)^{1/n_0}$, whose values are shown in Fig. 11. Unknown parameters of $1-f$, R_t, and s are included in Eq. (8). Among them, $1-f$ and s are expressed in the combined form of $(1-f)(L/s)^{1/n_0}$ in Eq. (8). Namely, the V-I curve is determined by the two parameter values of $(1-f)(L/s)^{1/n_0}$ and R_t, not by the three parameters of $1-f$, s, and R_t. In the analysis in Secs. V A–V C above, we used a fixed value of $s=0.1$ μm to estimate $1-f$ and R_t by curve-fitting with measured V-I curve. As $1-f$ and R_t are obtained as to best-fit the measured V-I curve for $s=0.1$ μm, the $(1-f)(L/s)^{1/n_0}$, calculated by the obtained $1-f$ and used s-value, and the obtained R_t also best-fit to the measured V-I curve. Even if other s-value ($s \ll L$) is used for analysis of a given V-I curve, the $(1-f)\times(L/s)^{1/n_0}$ and R_t are the same since they are obtained as to best-fit to the V-I curve. Namely, though the $1-f$ and s are treated as separated values in the procedure, $(1-f)(L/s)^{1/n_0}$ is determined uniquely regardless the s-value ($s \ll L$) due to the nature of curve-fitting. Accordingly, the results obtained under a fixed $s=0.1$ μm {V-I curves (Fig. 4), resistance R_t [Fig. 6(b)], I_c [Fig. 7(a)], n-value [Fig. 7(b)], $n-I_c$ relation [Fig. 7(c)], I_s (Fig. 8), V_s (Fig. 9), and $(1-f)(L/s)^{1/n_0}$ (Fig. 11)} are retained for any s-value ($s \ll L$).

As stated above, due to the nature of curve-fitting, even if other s-value is used, the V-I curve can be reproduced and cracking-induced shunting behavior can be revealed by obtaining $(1-f)(L/s)^{1/n_0}$ and R_t. However, as long as s-value is unknown, $1-f$ cannot be obtained precisely. The influence of s-value on $1-f$ is examined below.

From the construction of Eqs. (8) and (6), $1-f$ varies with s-value. The $1-f$ values in Figs. 6(a) and 10 are valid only for $s=0.1$ μm. If other s-value is used, different results are obtained. As $(1-f)(L/s)^{1/n_0}$ is uniquely obtained, the influence of s-value on $1-f$ can be examined by substituting s-value and the known values of $L=45$ mm and $n_0=39.6$ into $(1-f)(L/s)^{1/n_0}$. For instance, for $s=1$ μm (ten times larger than 0.1 μm) and 10 μm (100 times larger than 0.1 μm), $1-f$ values become larger by 1.06 and 1.12 times, respectively, in comparison with the $1-f$ value for $s=0.1$ μm. Even if the used s-value is different by 100 times from 0.1 μm, the difference in $1-f$ is around 10%. Though $1-f$ value is dependent on s-value, it is not so sensitive to s-value.

Downloaded 25 Nov 2010 to 130.54.110.31. Redistribution subject to AIP license or copyright; see http://jap.aip.org/about/rights_and_permissions

VI. CONCLUSIONS

(1) The experimental results were analyzed with the model of Fang *et al.*, in which the current shunting under existence of a crack is incorporated. In application, the arrayed multiple cracks was treated as a single equivalent crack. The experimentally measured variations in *V-I* curve, critical current, and *n*-value with increasing applied strain and the correlation of *n*-value to critical current were described well by this model with replacement of multiple cracks by a single equivalent crack.

(2) At critical current under a criterion of 1 μV/cm, most of the imposed current is transported by the noncracked part of the superconducting layer, and the voltage is developed mostly in the cracked region in advance of development of voltage in the noncracked region.

(3) Critical current under existence of partial crack decreases almost linearly with decreasing modified ratio of noncracked area to overall cross-sectional area of superconducting layer.

ACKNOWLEDGMENTS

The authors wish to express their gratitude to The Ministry of Education, Culture, Sports, Science, and Technology, Japan for the grant-in-aid (Grant No. 22360281).

[1] D. Uglietti, B. Seeber, V. Abächerli, W. L. Carter, and R. Flükiger, Supercond. Sci. Technol. **19**, 869 (2006).
[2] D. C. Larbalestier, A. Gurevich, D. M. Feldmann, and A. A. Polyanskii, Nature (London) **414**, 368 (2001).
[3] V. Selvamanickam, Y. Chen, X. Xiong, Y. Xie, X. Zhang, A. Rar, M. Martchevskii, R. Schimidt, K. Lenseth, and J. Herrin, Physica C **468**, 1504 (2008).
[4] A. P. Malozemoff, S. Fleishler, M. Rupich, C. Thime, X. Ki, Q. Zhnag, A. Otto, J. Maguire, D. Folts, J. Yuan, H.-P. Kraemer, W. Schmidt, M. Wohlfart, and H.-W. Neumueller, Supercond. Sci. Technol. **21**, 034005 (2008).
[5] M. Sugano, K. Osamura, W. Prusseit, R. Semerad, K. Itoh, and T. Kiyoshi, Supercond. Sci. Technol. **18**, S344 (2005).
[6] M. Sugano, K. Osamura, W. Prusseit, R. Semerad, T. Kuroda, K. Itoh, and T. Kiyoshi, IEEE Trans. Appl. Supercond. **15**, 3581 (2005).
[7] M. Sugano, T. Nakamura, T. Manabe, K. Shikimachi, N. Hirano, and S. Nagaya, Supercond. Sci. Technol. **21**, 115019 (2008).
[8] K. Osamura, M. Sugano, S. Machiya, H. Adachi, S. Ochiai, and M. Sato, Supercond. Sci. Technol. **22**, 065001 (2009).
[9] D. C. van der Laan, J. W. Ekin, J. F. Douglas, C. C. Clickner, T. C. Stauffer, and L. F. Goodrich, Supercond. Sci. Technol. **23**, 072001 (2010).
[10] D. C. van der Laan and J. W. Ekin, Appl. Phys. Lett. **90**, 052506 (2007).
[11] D. C. van der Laan, T. J. Haugan, P. N. Barnes, D. Abraimov, F. Kametani, D. C. Larbalestier, and M. W. Rupich, Supercond. Sci. Technol. **23**, 014004 (2010).
[12] H.-S. Shin, K.-H. Kim, J.-R. Dizon, T.-Y. Kim, R.-K. Ko, and S.-S. Oh, Supercond. Sci. Technol. **18**, S364 (2005).
[13] N. Cheggour, J. W. Ekin, Y.-Y. Xie, V. Selvamanickam, C. L. H. Thieme, and D. T. Verebelyi, Appl. Phys. Lett. **87**, 212505 (2005).
[14] N. Cheggour, J. W. Ekin, C. L. H. Thieme, Y.-Y. Xie, V. Selvamanickam, and R. Feenstra, Supercond. Sci. Technol. **18**, S319 (2005).
[15] W. Prusseit, R. Nemetschek, C. Hoffmann, G. Sigl, A. Lümkemann, and H. Kinder, Physica C **426–431**, 866 (2005).
[16] W. Prusseit, R. Semerad, K. Irgmaier, and G. Sigl, Physica C **392–396**, 1225 (2003).
[17] Y. Fang, S. Danyluk, and M. T. Lanagan, Cryogenics **36**, 957 (1996).
[18] A. Nyilas, Supercond. Sci. Technol. **18**, S409 (2005).
[19] J. K. Shin, S. Ochiai, H. Okuda, M. Sugano, and S. S. Oh, Supercond. Sci. Technol. **21**, 115007 (2008).
[20] Y. Miyoshi, E. P. A. Van Lanen, M. M. Dhallé, and N. Nijhuits, Supercond. Sci. Technol. **22**, 085009 (2009).

Downloaded 25 Nov 2010 to 130.54.110.31. Redistribution subject to AIP license or copyright; see http://jap.aip.org/about/rights_and_permissions